Catal Lett (2008) 122:131–137
DOI 10.1007/s10562-007-9358-4

Photooxidation of Polycyclic Aromatic Hydrocarbons over $NaBiO_3$ under Visible Light Irradiation

Jiahui Kou · Haitao Zhang · Zhaosheng Li · Shuxin Ouyang · Jinhua Ye · Zhigang Zou

Received: 27 September 2007 / Accepted: 16 November 2007 / Published online: 4 December 2007

Abstract The $NaBiO_3$ samples ($NaBiO_3 \cdot nH_2O$) used in photooxidation of polycyclic aromatic hydrocarbon were obtained through heating $NaBiO_3 \cdot 2H_2O$. The samples were characterized by X-ray diffractometer and ultraviolet-visible spectrophotometer. The photooxidation of anthracene and Benz[a]anthracene over $NaBiO_3 \cdot nH_2O$ was investigated, respectively. The intermediates were analysed by gas chromatography-mass spectrometer. The results indicated that the prepared $NaBiO_3$ samples showed considerable photooxidation activity and stability for PAHs degradation under visible light irradiation. The possible reaction pathways of the decomposition of the two polycyclic aromatic hydrocarbons were proposed.

Keywords Polycyclic aromatic hydrocarbon · $NaBiO_3$ · Photooxidation · Anthracene · Benz[a]anthracene

Electronic supplementary material The online version of this article (doi:10.1007/s10562-007-9358-4) contains supplementary material, which is available to authorized users.

J. Kou · H. Zhang · Z. Li · S. Ouyang · Z. Zou (✉)
Department of Physics, Eco-materials and Renewable Energy Research Center (ERERC), Nanjing University, Nanjing 210093, China
e-mail: zgzou@nju.edu.cn

J. Kou · H. Zhang · Z. Li · S. Ouyang
Department of Materials Science and Engineering, Nanjing University, Nanjing 210093, China

J. Kou · H. Zhang · Z. Li · S. Ouyang · Z. Zou
National Laboratory of Solid State Microstructures, Nanjing University, Nanjing 210093, China

S. Ouyang · J. Ye
Photocatalytic Materials Center, National Institute for Materials Science (NIMS), 1-2-1 Sengen, Tsukuba, Ibaraki 305-0047, Japan

1 Introduction

Polycyclic aromatic hydrocarbons (PAHs) and their derivatives, as widespread and high toxic pollutants, come from incomplete combustion of organic compounds in foods, fossil fuels and cigarettes, etc. [1] They are difficult to decompose in natural environment due to their stable structure and low water solubility. Furthermore, the intensive industrial development during the past two hundred years has resulted in the increase of PAHs emission sources. Sixteen PAHs including anthracene (ANT), Benz[a]anthracene (Bz[a]A), phenanthrene, fluorene, etc, are listed by the US EPA as priority pollutants that should be monitored in the environment [2]. Therefore, the degradation of PAHs has attracted more and more attentions over the last two decades [3–6].

Recently, photocatalytic reactions over semiconductors have been applied to remove such organic pollutants, which can utilize the inexpensive and inexhaustible solar energy [7–15]. Almost all of the semiconductor photocatalysts available so far for PAHs photocatalytic decontamination are dominated by titania (TiO_2) [7–14]. Even though TiO_2 is a chemically and biologically inert, photostable and cheap photocatalyst, it has a fatal drawback that it absorbs only UV light, and therefore it can only utilize less than 5% of solar energy. In order to improve the utilization efficiency of solar energy, it is very important to develop stable and active photocatalysts which could work under visible light irradiation.

Some new catalysts have been reported for the activity of organic contaminants photodegradation under visible light irradiation [15–21]. However, to the best of our knowledge, few visible light responded photocatalyst has been used to investigate the photodegradation of PAHs expect $BiVO_4$ [15]. Especially, report about

photodegradation of solid state PAHs on photocatalyst is scarce. $NaBiO_3$ exhibits the visible light absorption because of its hybridized valence band (VB) by O 2p and Bi 6s orbitals. The large dispersion of the hybridized sp orbitals in the conduction band increases the mobility of the photoexcited electrons, thus suppressing the recombination of photoexcited electron-hole pairs and enhancing activities [21]. We have reported its high activities for the decomposing of Methylene Blue and 2-propanol under visible light irradiation [21]. However, no work has been reported about the photodegradation of other organic compounds over $NaBiO_3$. Consequently, it is important to study the photodegradation of PAHs over $NaBiO_3$ not only for the research of PAHs decomposition but also for the development of new applications of $NaBiO_3$. In addition, the treatment condition of $NaBiO_3$ needs to be investigated in detail for obtaining optimal activity.

Herein, the photooxidations of PAHs over the $NaBiO_3$ samples were investigated. ANT and Bz[a]A dispersed widely in the environment were chosen as low-molecular-weight and high-molecular-weight model pollutant, respectively. $NaBiO_3$ samples used in photooxidation reaction were obtained by heating $NaBiO_3 \cdot 2H_2O$. The intermediates and products were analyzed by gas chromatography-mass spectrometer (GC-MS). The effects of irradiation time, cut-off wavelength and amount of $NaBiO_3$ on the photodegradation of ANT and Bz[a]A were studied. The possible reaction pathways were also proposed. The results would provide useful information for the research of PAHs decomposition and the development of new application of $NaBiO_3$.

2 Experimental

The $NaBiO_3$ samples were prepared by heating commercial $NaBiO_3 \cdot 2H_2O$ (Wako Pure Chemicals Industries Ltd, Japan) in air. The surface areas of the samples were determined by BET measurement (TriStar-3000, Micromeritics, America). SAMPLE-A, SAMPLE-B and SAMPLE-C mentioned in this study were prepared as follows. The sample heated at 175 °C for 2 h was denoted as SAMPLE-A. The suspended liquid of SAMPLE-A was stirred in dark for 8 h, and then SAMPLE-B was obtained after the powder was centrifuged and dried. The SAMPLE-A after ANT photodegradation for 8 h was centrifuged and dried to gain the sample represented as SAMPLE-C. The crystal structures of $NaBiO_3$ samples were investigated with an X-ray diffractometer (XRD) (Utilma III Tokyo, Japan). The optical absorption spectra of prepared $NaBiO_3$ samples were obtained by using an ultraviolet-visible diffuse reflectance spectrophotometer (UV-vis) (Shimadzu UV-2550, Japan). Acetone, dichloromethane, TiO_2 (anatase), Na_2SO_4, Bz[a]A, and ANT were all analytical grade. Acetone and dichloromethane were purified by distillation, and other reagents were used without further purification.

The irradiation system consisted of a 300 W Xe arc lamp, a cut-off filter, a 100 mL quartz reaction cell, and a water cooler trough (preventing the thermal catalytic effect). In the liquid–solid experiments, 0.003 g PAH was firstly dissolved in the solution consisted of 20 mL water and 40 mL acetone. Then the solution of PAH was added into the quartz cell containing a certain amount of $NaBiO_3$ sample. The suspension was magnetically stirred in the dark for several hours before irradiation to ensure the establishment of an adsorption/desorption equilibrium of PAHs on the sample surface. Then, the reactor was immersed in ice–water mixture, and was irradiated through a cut-off filter. After the reaction, the slurry of reaction mixture was taken out and centrifuged to remove $NaBiO_3$ sample. Afterwards, the products were extracted by dichloromethane, and the dichloromethane layer was dried by anhydrous sodium sulfate for GC (Agilent 6890N, USA) and GC-MS (Agilent 6890N/5973I, USA) analysis. Products were quantitative analyzed by GC. The GC was equipped with flame ionization detection (GC/FID) and split/splitless injector. The injection mode was split injection with the split ratio of 16.5:1. An HP-5 column was used for separation (30 m, 0.25 mm I. D., 0.25 μm film thickness). The temperature program started at 60 °C and was held for 5 min. The oven was heated to 280 °C at a rate of 15 °C min^{-1}, and then the temperature was maintained for 5 min. The solvent delay time was set to 4.3 min. All quantifications and calculations were based on an external standard and the use of calibration curve. The intermediates were identified by comparing the mass spectra with data in the NIST 02 library. The operation condition of GC instrument was the same as that mentioned above. Mass spectra were recorded at 1 scan s^{-1} under electron impact at 70 eV, mass range 30–350 amu.

If no special explain was presented, the irradiation wavelength was longer than 420 nm, and the sample used in the photodegradation of PAHs was SAMPLE-A. In order to study the cut-off wavelength dependence of PAHs degradation, the cut-off filters of 420, 440, 480, 520, 560 and 660 nm were used; the amount of SAMPLE-A and TiO_2 are both 0.05 g; and the irradiation time of ANT and Bz[a]A was 6 and 2 h, respectively. Time courses studies for degradation of PAHs were carried out by using 0.02–0.3 g SAMPLE-A. The repeated degradation experiments of ANT were carried out to investigate the stability of SAMPLE-A. The original SAMPLE-A and ANT dose was 0.3 g and 0.003 g, respectively. In this experiment, the conversion of ANT was analyzed by disposal all of the reaction remainder, using the disposal method mentioned above. Then, the residual $NaBiO_3$ was used in the next

experiment. In the beginning of each circle, PAHs was added into the reactor to keep the original PAHs dose of 0.003 g. The same experiments were performed for four runs.

In the photodegradation experiments of solid state PAHs on SAMPLE-A, 0.003 g PAHs and 0.1 g SAMPLE-A was homogeneous mixed using an agate mortar. After given interval, the products were extracted by dichloromethane for GC-MS analysis.

3 Results and Discussion

Figure 1 displays the XRD patterns of commercial $NaBiO_3$, SAMPLE-A, SAMPLE-B and SAMPLE-C. The XRD pattern of commercial $NaBiO_3$ was in good agreement with $NaBiO_3 \cdot 2H_2O$ (JCPDS 30–1160) [22]. SAMPLE-A was identified with the dehydrated phase of $NaBiO_3 \cdot nH_2O$ (JCPDS 30–1161) [22], and it well-crystallized into an ilmenite structure (space group R-3). Comparing the patterns of SAMPLE-A with SAMPLE-B, only tiny change could be observed, and the pattern of SAMPLE-B was quite different from $NaBiO_3 \cdot 2H_2O$. It can be inferred that the crystal water of $NaBiO_3 \cdot 2H_2O$, which was lost in the process of heating, was difficult to regain in water. Moreover, the XRD pattern of SAMPLE-B was similar with that of SAMPLE-C. These results indicated that SAMPLE-A was relatively stable in water and under light irradiation. The XRD patterns of $NaBiO_3$ samples heated in different conditions are showed in Figure S1. No obvious difference was observed between these XRD patterns.

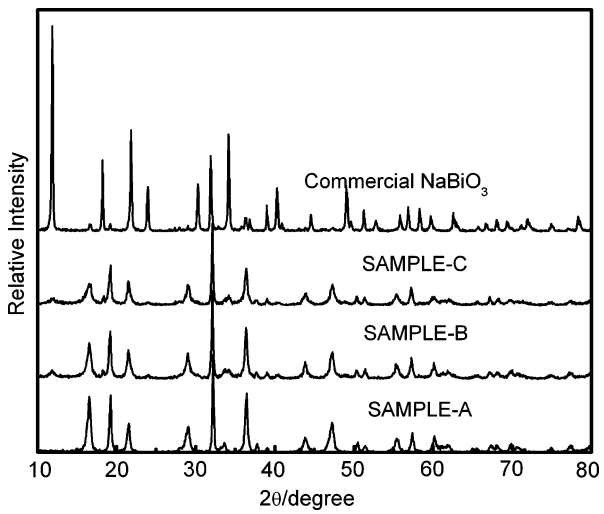

Fig. 1 XRD patterns of the samples. The commercial $NaBiO_3 \cdot nH_2O$ was heated at 175 °C for 2 h to obtain SAMPLE-A. The suspended liquid of SAMPLE-A was stirred in dark for 8 h, and then SAMPLE-B was obtained after the powder was centrifuged and dried. The SAMPLE-A after ANT photodegradation for 8 h was centrifuged and dried to gain the sample represented as SAMPLE-C

The experimental results about ANT photodegradation on $NaBiO_3$ samples which were heated in different conditions, were displayed in Table 1. The conversion of ANT photooxidated over $NaBiO_3$ without pretreatment was 20.9%. The activities of $NaBiO_3$ samples were improved by optimizing heating conditions. There was an optimal heating time for the activity of $NaBiO_3$ samples at every temperature, which was 4 h at 150 °C, 2 h at 175 °C, 1 h at 200 °C and 1 h at 250 °C, respectively. Moreover, there was also an optimal heating temperature for the activity of $NaBiO_3$ at every time, and the optimal temperature would decrease with the increment of heating time. As a result, the conversion of ANT was the highest, 56.6%, when $NaBiO_3$ was heating at 175 °C for 2 h. The BET measurement showed that the values of surface area of all the samples were similar (5.6–5.9 $m^2\ g^{-1}$, see Table 1), indicating that the difference in activities should not be caused by the surface area. We consider that the difference of the activity of $NaBiO_3$ samples possibly associated with the lost crystal water of $NaBiO_3$, and the further work is in progress.

As shown in Fig. 2, the UV-vis absorption edge of $NaBiO_3 \cdot 2H_2O$ red shifted after heating. The UV-vis absorption edge of SAMPLE-A was around 470 nm due to

Table 1 ANT photodegradtion on $NaBiO_3$ samples which were heated in different condition. Reaction conditions: $\lambda > 420$ nm, the amount of ANT was 0.003 g, reaction time was 6 h

Sample	Heating Temperature (°C)	Heating Time (h)	Conversion of ANT (%)	Surface area ($m^2\ g^{-1}$)
Original $NaBiO_3$	–	0	20.9	5.7
$NaBiO_3$-150-1h	150	1	32.4	5.8
$NaBiO_3$-150-2h	150	2	40.5	5.7
$NaBiO_3$-150-3h	150	3	46.7	5.7
$NaBiO_3$-150-4h	150	4	50.3	5.8
$NaBiO_3$-150-6h	150	6	45.3	5.7
$NaBiO_3$-175-1h	175	1	48.2	5.9
$NaBiO_3$-175-2h	175	2	56.6	5.8
$NaBiO_3$-175-3h	175	3	50.4	5.7
$NaBiO_3$-175-4h	175	4	45.3	5.8
$NaBiO_3$-200-1h	200	1	40.9	5.8
$NaBiO_3$-200-2h	200	2	38.2	5.8
$NaBiO_3$-200-3h	200	3	34.5	5.7
$NaBiO_3$-200-4h	200	4	29.1	5.6
$NaBiO_3$-250-1h	250	1	15.7	5.8
$NaBiO_3$-250-2h	250	2	14.3	5.7
$NaBiO_3$-250-3h	250	3	10.2	5.8
$NaBiO_3$-250-4h	250	4	5.1	5.7

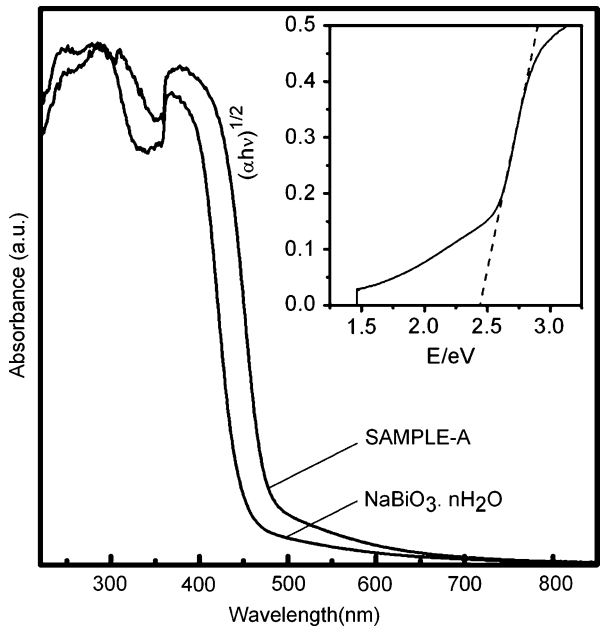

Fig. 2 UV-vis absorption spectra of the samples. Inset: the calculation diagram of SAMPLE-A band gap

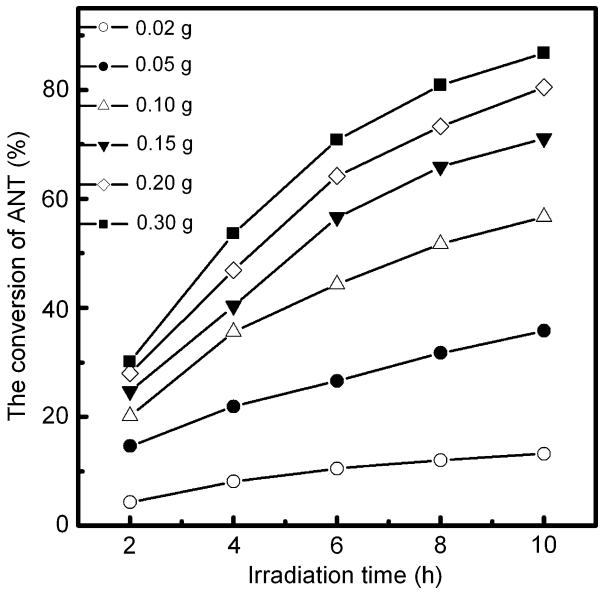

Fig. 3 Effect of the amount of SAMPLE-A on the conversion of ANT under visible light irradiation. Reaction conditions: $\lambda > 420$ nm, the amount of ANT was 0.003 g

the band gap transition. There was a long tail up to 700 nm, which may be caused by the lattice defects, such as oxygen vacancies [21]. From the onset of the absorption edge, the optical band gap was estimated by the following equation,

$$\alpha hv = A\left(hv - E_g\right)^n$$

in which α, v, A, and E_g is absorption coefficient, light frequency, proportionality constant, and band gap, respectively [23]. In the equation, n depends on the characteristics of the transition in a semiconductor. The value of n for the $NaBiO_3$ was determined as 2 (see Fig. 2). The band gap of SAMPLE-A is determined to be about 2.45 eV.

The photooxidation of ANT was investigated using the different amount of SAMPLE-A, and the experimental results are shown in Fig. 3. The conversion of ANT was enhanced with the prolonging of irradiation time and the increase of the dose of SAMPLE-A. The conversion of ANT was only about 4.6% when the amount of SAMPLE-A was 0.02 g and the reaction time was 2 h. And the conversion of ANT reached 86.8% at 10 h when the amount of SAMPLE-A was 0.3 g. It is very interesting to find that the conversion of ANT increased more rapidly with the increment of SAMPLE-A, when the amount of SAMPLE-A was small. The possible reason was that SAMPLE-A was opacity, so it could block off part of light. The availability ratio of light was therefore higher when the dose of SAMPLE-A was small.

The wavelength dependence of photooxidation activity of a semiconductor is often used to judge whether a reaction is really driven by light or not. Figure 4 displays the cut-off wavelength dependence of the conversion of ANT containing SAMPLE-A or TiO_2. The obvious decrease in the photooxidation activity of SAMPLE-A was observed when a 480 nm (nearly corresponding to the onset of absorption edge of SAMPLE-A) cut-off filter was used. In order to clarify the role of SAMPLE-A, the self-decomposition experiment was also carried out under the same condition. The conversion of ANT was 0.3% when SAMPLE-A was

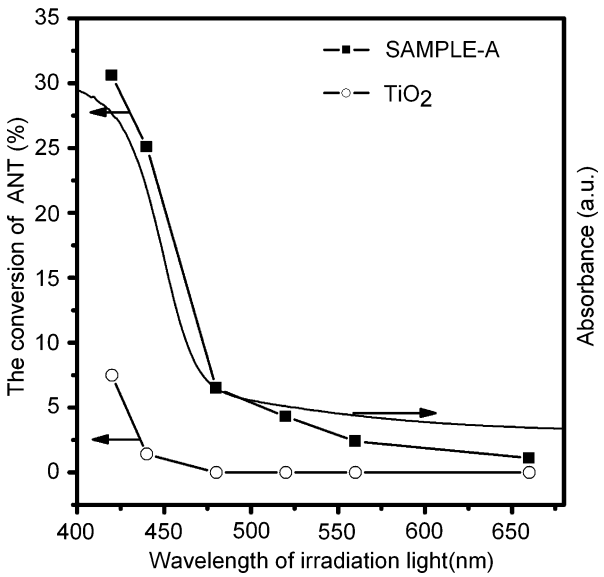

Fig. 4 Cut-off wavelength dependence of the conversion of ANT. Reaction conditions: reaction time was 6 h, the amount of ANT, TiO_2 and SAMPLE-A was 0.003 g, 0.05 g and 0.05 g, respectively

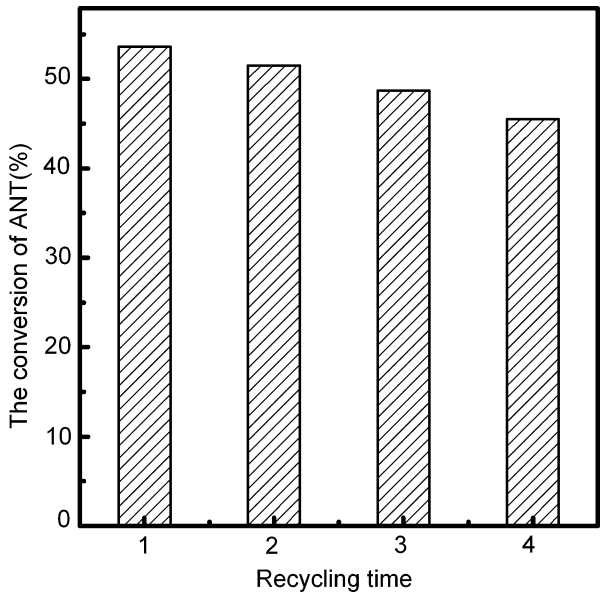

Fig. 5 The evaluation of the durability of SAMPLE-A photooxidation from the repeatable degradation of ANT. Reaction conditions: reaction time of each cycle was 4 h, the amount of ANT was 0.003 g, and the initial amount of SAMPLE-A was 0.3 g

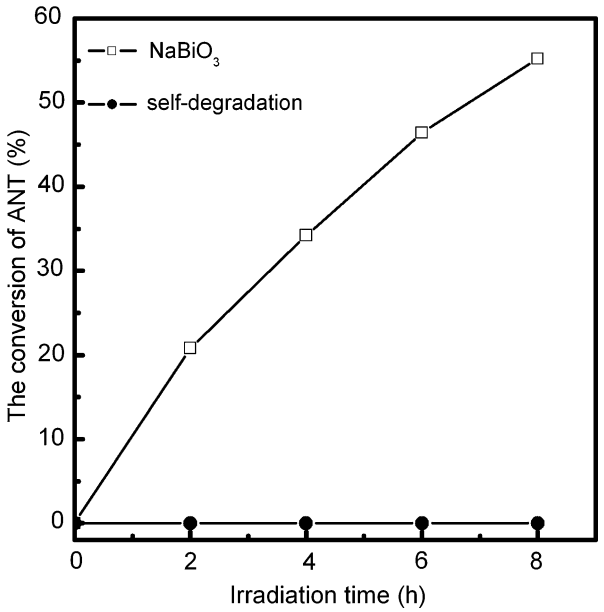

Fig. 6 The conversion of solid state ANT on SAMPLE-A under visible light irradiation. Reaction conditions: $\lambda > 420$ nm, the amount of ANT and SAMPLE-A was 0.003 g and 0.1 g, respectively

absent, indicating that the high degradation efficiency of ANT should be attributed to the effect of SAMPLE-A. In comparison of SAMPLE-A with TiO_2-used solution, it is obvious that the conversion of ANT using SAMPLE-A was much higher than that of using TiO_2.

The durability of SAMPLE-A for ANT photooxidation was also investigated, as shown in Fig. 5. The conversion of ANT was 53.6% in the first cycle, and 45.5% in the fourth run, suggesting the slight decline of conversion in photooxidation process. However, 32% of the SAMPLE-A was lost in the separation process. Consequently, the degradation efficiency of ANT in the fourth run should be compared with the degradation rate of ANT on 0.2 g SAMPLE-A. As Fig. 3 shows, the conversion of ANT was 46.9% when the dose of SAMPLE-A was 0.2 g. These results suggested that SAMPLE-A could keep considerable stable under visible light irradiation.

Figure 6 illustrates the photodegradation of ANT on SAMPLE-A without solvent. Under visible light irradiation, the conversion of ANT increased with prolonging of irradiation time in the presence of SAMPLE-A. The conversion of ANT reached to 55.2% after 8 h irradiation. The experiment of self-degradation of ANT was also carried out under the same condition to clarify the role of SAMPLE-A. As we can see from Fig. 6, ANT could not self-degrade under visible light irradiation at 8 h. SAMPLE-A is therefore favorable for solid phase photodegradation of ANT.

The GC-MS analysis results (see Figure S2 and S3) indicated that anthraquinone was the main degradation product of ANT over SAMPLE-A under visible light irradiation. In addition, anthrone and 1-hydroxyanthracene were also identified. However, only a degradation product, anthraquinone, was detected when SAMPLE-A was absent. In photolysis process, ANT was directly excited by light and reacted with singlet oxygen to form 9,10-endoperoxyanthracene, and then rearrangement and further oxidation of the endoperoxide leaded to the formation of anthraquinone. As a result, anthrone was never produced in photolysis process [24, 25]. As mentioned above, we can conclude that anthrone, one of the products, was generated from ANT photooxidation over SAMPLE-A. The possible photooxidation pathway of ANT over the SAMPLE-A under visible light irradiation is illustrated in Scheme 1. Firstly, 9 or 9 & 10 position of ANT was oxidized resulting

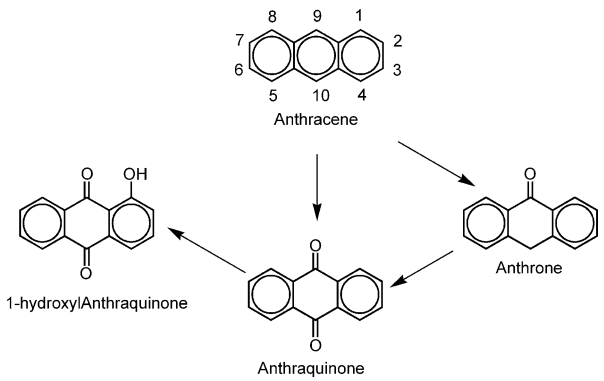

Scheme 1 Degradation pathway of ANT in the SAMPLE-A suspended solution under visible light irradiation

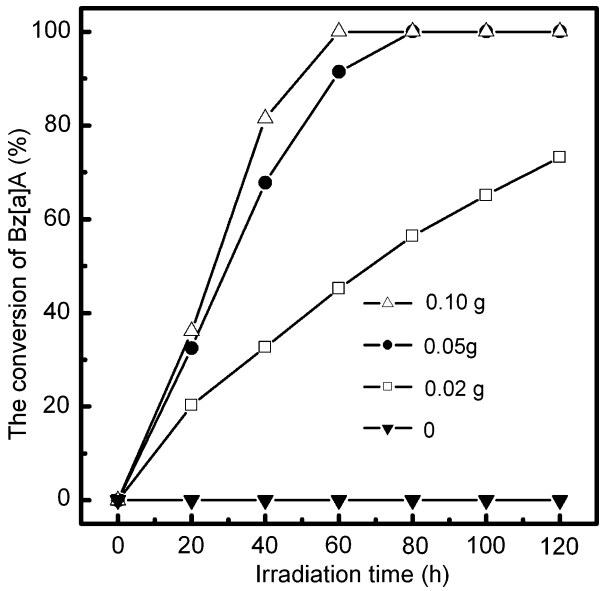

Fig. 7 The effect of the amount of SAMPLE-A on the conversion of Bz[a]A under visible light irradiation. Reaction conditions: $\lambda > 420$ nm, the amount of Bz[a]A was 0.003 g

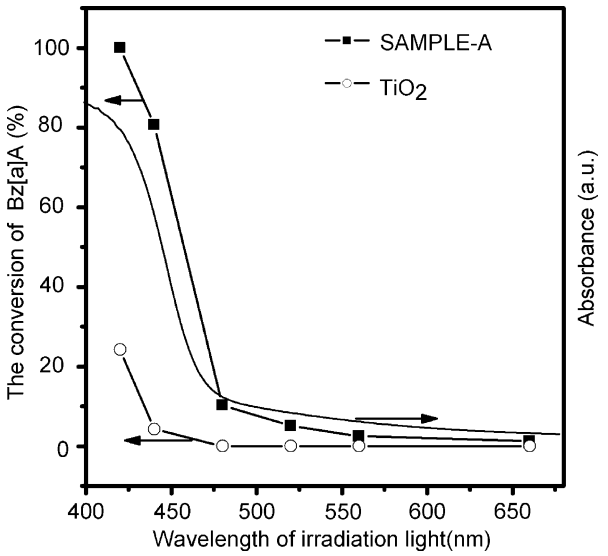

Fig. 8 Cut-off wavelength dependence of the conversion of Bz[a]A. Reaction conditions: reaction time was 2 h, the amount of ANT, TiO_2 and SAMPLE-A was 0.003 g, 0.05 g and 0.05 g, respectively

in the formation of anthrone and anthraquinone, then anthraquinone was oxidized to form 1-hydroxyanthracene.

The conversion of Bz[a]A in the SAMPLE-A suspended solution under visible light irradiation was illustrated in Fig. 7. In the experiment of SAMPLE-A-free, no Bz[a]A was degraded after 120 min irradiation. The conversion of Bz[a]A was enhanced with the increment of the irradiation time in the presence of SAMPLE-A. The conversion was about 20.3% at 20 min and 73.2% at 120 min when the amount of SAMPLE-A was 0.02 g. The degradation rate of Bz[a]A was improved with the increase of the dose of SAMPLE-A. When the amount of SAMPLE-A was 0.1 g, the conversion of Bz[a]A reached to 100% at 60 min. The wavelength dependence of Bz[a]A photooxidation is displayed in Fig. 7. The conversion of Bz[a]A decreased obviously when a 480 nm cut-off filter was used, which was in agreement with the onset of absorption edge of SAMPLE-A. The wavelength dependence results of Bz[a]A photooxidation further proved that the oxidation of PAHs on SAMPLE-A were driven by light, as well as the result of ANT photooxidation. In comparison of SAMPLE-A with TiO_2-used solution, the conversion of Bz[a]A in the SAMPLE-A-used solution was much higher than the TiO_2-used solution. The photodegradation of solid state Bz[a]A on the SAMPLE-A was also investigated under visible light irradiation. (Fig. 8). Figure 9 shows the conversion of Bz[a]A in the presence or absence of SAMPLE-A. The conversion of Bz[a]A on the SAMPLE-A increased with the prolonging of reaction time. And it reached to 65.2% at 8 h irradiation in the presence of SAMPLE-A, while Bz[a]A could not be oxidated without SAMPLE-A under the same condition.

Benz[a]anthrancene-7-12-dione was identified by GC-MS (see Figure S4 and S5) in the reaction residue. A possible reaction pathway was proposed, which was similar to that of anthrance as described above, as shown in Scheme 2. Bz[a]A was firstly photooxidated to produce monohydroxybenz[a]anthrancene, and monohydroxybenz[a]anthrancene was then oxidated to produce Benz[a]anthrancene-7-12-dione.

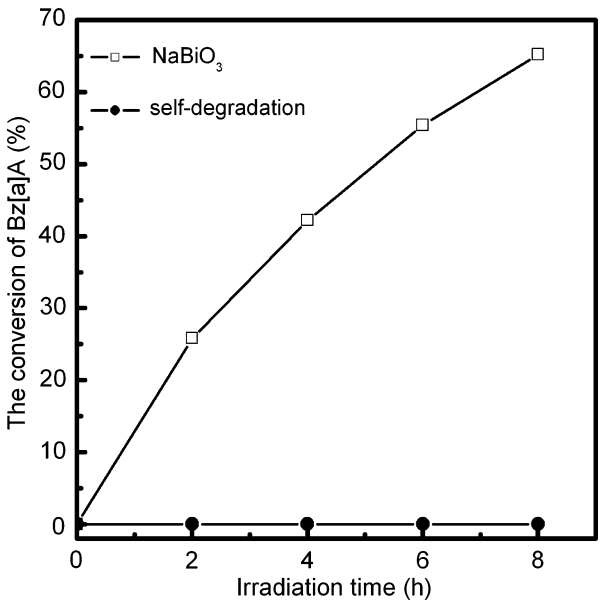

Fig. 9 The conversion of solid state Bz[a]A on SAMPLE-A under visible light irradiation. Reaction conditions: $\lambda > 420$ nm, the amount of Bz[a]A and SAMPLE-A was 0.003 g and 0.1 g, respectively

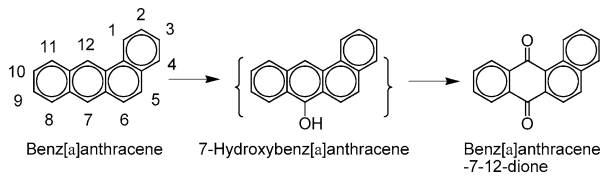

Scheme 2 Degradation pathway of Bz[a]A in the SAMPLE-A suspended solution under visible light irradiation

4 Conclusion

In conclusion, the $NaBiO_3$ samples were prepared by heating $NaBiO_3 \cdot 2H_2O$ in different conditions, and the photooxidations of PAHs on the $NaBiO_3$ samples were investigated in liquid–solid and solid–solid reactions. The results indicated that some $NaBiO_3$ samples have considerable photooxidation ability for the degradation of PAHs under visible light irradiation, and the sample (SAMPLE-A) heated at 175 °C for 2 h, had the optimal activity. SAMPLE-A could keep relatively stability in water under light irradiation. The products of photooxidation of PAHs were identified and quantified by GC-MS and GC, respectively. Anthraquinone, which is biodegradable, was detected as a major product of ANT photooxidation along with small amounts of anthrone and 1-hydroxyanthracene. Benz[a]anthrancene-7-12-dione was identified as the main product of Bz[a]A photooxidation.

Acknowledgments The authors gratefully acknowledge the financial support from the National High Technology Research Project of China (No. 2006AA052113), the National Natural Science Foundation of China (No. 20528302), and the Jiangsu Provincial Natural Science Foundation of China (No. BK2006718). The National Basic Research Program of China (No. 2007CB613300) is also gratefully acknowledged. Prof. Z. G. Zou and T. Yu would like to thank the Jiangsu Provincial Talent Scholars Program.

References

1. Boonchan S, Britz ML, Stanley G (2000) Appl Environ Microb 66:1007
2. Callahan MA, Slimak MW, Gabelc NW, May IP, Fowler CF, Freed JR, Jennings P, Durfee RL, Whitmore FC, Maestri B, Mabey WR, Holt BR and Gould C (1979) US Environmental Protection Agency, Washington, DC
3. Guessan A, Carignan T, Nyman M (2004) Environ Sci Technol 38:1554
4. An Y, Carraway ER (2002) Water Res 36:309
5. Sigman ME, Schuler PF, Ghosh MM, Dabestani RT (1998) Environ Sci Technol 32:3980
6. Guessan AL, Carignan T, Nyman MC (2004) Environ Sci Technol 38:1554
7. García-Martínez MJ, Canoira L, Blázquez G, Riva ID, Alcántara R, Llamas JF (2005) Chem Eng J 110:123
8. Rababah A, Matsuzawa S (2002) Chemosphere 46:49
9. Garcia T, Solsona B, Cazorla-Amorós D, Linares-Solano Á, Taylor SH (2006) Appl Catal B 62:66
10. Pal B, Sharon M (2000) J Mol Catal A 160:453
11. Wen S, Zhao J, Sheng G, Fu J, Peng P (2003) Chemosphere 50:111
12. Lin H, Valsaraj KT (2003) J Hazard Mater 99:203
13. Roméas V, Pichat P, Guillard C, Chopin T, Lehaut C (1999) Ind Eng Chem Res 38:3878
14. Beltrán FJ, Rivas FJ, Gimeno O, Carbajo M (2005) Ind Eng Chem Res 44:3419
15. Kohtani S, Tomohiro M, Tokumura K, Nakagaki R (2005) Appl Catal B 58:265
16. Kudo A, Omori K, Kato H (2004) J Am Chem Soc 129:8912
17. Tang J, Zou Z, Ye J (2004) Catal Lett 92:53
18. Kohtani S, Koshiko M, Kudo A, Tokumura K, Ishigaki Y, Toriba A, Hayakawa K, Nakagaki R (2003) Appl Catal B 46:573
19. Ito S, Thampi KR, Comte P, Liska P, Grätzel M (2005) Chem Commun 5:268
20. Torres-Martínez CL, Kho R, Mian OI, Mehral RK (2001) J Colloid Interf Sci 240:525
21. Kako T, Zou Z, Katagiri M, Ye J (2007) Chem Mater 19:198
22. International Centre for Diffraction Data. Powder Diffraction File; McClune WF, Mrose ME, Post B, Weissmann S, McMurdie HF (eds), JCPDS International Centre for Diffraction Date: Swarthmore, PA, 1987; Inorganic vols. 29–30, p 957
23. Butler MA (1977) J Appl Phys 48:1914
24. Schmidt R, Schaffner K, Trost W, Brauer HD, Masaaki Hosomi (1984) J Phys Chem 88:956
25. Sigman ME, Zingg SP, Pagni RM, Burns JH (1991) Tetrahedron Lett 32:5737
26. Jensen TE, Hltes RA (1883) Anal Chem 55:594
27. David B, Riguier D (2002) Ultrason Sonochem 9:45